HIPO – A High-speed Imaging Photometer for Occultations

E. W. Dunham[a], J. L. Elliot[a,b], T. A. Bida[a], and B. W. Taylor[a]

[a]Lowell Observatory, 1400 W. Mars Hill Road, Flagstaff, AZ 86001

[b]Department of Earth, Atmospheric and Planetary Science, MIT 54-422, 77 Massachusetts Ave., Cambridge, MA 02139

ABSTRACT

HIPO is a special purpose instrument for SOFIA, the Stratospheric Observatory For Infrared Astronomy. It is a high-speed, imaging photometer that will be used for a variety of time-resolved precise photometry observations, including stellar occultations by solar system objects and transits by extrasolar planets. HIPO has two independent CCD detectors and can also co-mount with FLITECAM, an InSb imager and spectrometer, making simultaneous photometry at three wavelengths possible. HIPO's flexible design and high-speed imaging capability make it well suited to carry out initial test observations on the completed SOFIA system, and to this end a number of additional features have been incorporated. Earlier papers have discussed the design requirements and optical design of HIPO. This paper provides an overview of the instrument, describes the instrument's features, and reviews the actual performance, in most areas, of the completed instrument.

Keywords: CCD, airborne, imaging, photometer, SOFIA

1. INTRODUCTION

HIPO is a first-light instrument for SOFIA that has been designed to support observations of stellar occultations[1] with SOFIA. This makes use of the deployment capability of SOFIA, its freedom from clouds, and the low scintillation noise observed in airborne photometry[2,3]. Occultation photometry involves time-resolved, and precisely time-tagged photometry, so HIPO naturally is capable of high-speed CCD imaging. As such HIPO is also ideally suited for use in other time-resolved precise photometry applications, such as observations of transits by extrasolar planets[4] and asteroseismological observations[5]. It is also inherently well suited for use in the SOFIA functional and performance test program and builds on our experience with image quality measurements on the Kuiper Airborne Observatory[6,7]. In fact, HIPO will be the first instrument aboard SOFIA and will be heavily involved in the test program.

The HIPO science program, design requirements, and implementation plan were described in an earlier paper[8] that is generally still correct, though some implementation approaches have changed. The details of the HIPO optical design were given in a subsequent paper[9] that remains the definitive optical design definition for the instrument. The purpose of the present paper is to describe the as-built instrument as it will first be used on SOFIA and to provide its measured performance based on lab work and ground-based telescope measurements.

For many of the science and SOFIA test applications of HIPO it will be desirable to have a simultaneous near-IR observing capability. This will be provided by co-mounting FLITECAM with HIPO on the SOFIA telescope. FLITECAM is an InSb-based imager/spectrometer for SOFIA being built by Ian McLean's group at UCLA[10]. The ability to co-mount FLITECAM has been included in the HIPO design from the beginning, and the final implementation of this capability will also be described here.

At present the telescope-mounted portion of the HIPO hardware is complete, and the final rack-mounted electronics are in operation, although they are not yet mounted in a flight rack with approved hardware. HIPO achieved its first light

Ground-based Instrumentation for Astronomy, edited by
Alan F. M. Moorwood, Masanori Iye, Proceedings of SPIE Vol. 5492
(SPIE, Bellingham, WA, 2004) · 0277-786X/04/$15 · doi: 10.1117/12.552152

observation in October, 2003 using the 1.8-meter Perkins telescope at Lowell. First light for the co-mounted HIPO and FLITECAM pair occurred in early May, 2004 using the same telescope. There are a number of small items in the mechanical area that still need work, notably a redesigned cold strap in the dewars. No effort has been made yet to optimize the noise performance. The control software is partially developed, and readout modes other than single frames have not been finished. Some performance characterization remains to be done. The SOFIA interface software is the primary activity at present in the software area.

2. REQUIREMENTS MATRIX

The final requirements for HIPO are listed in Table 1, together with the verification approach and the actual value found for those cases where the value has been determined. A few comments relating to Table 1 follow here, but in-depth discussion of mechanical and optical performance is deferred to Section 4.

The HIPO blue channel optics allow operation from the UV cutoff at 300 nm to 650 nm while the red channel operates from 400-1100 nm.. Each channel has an 8-position filter wheel which is also available in the bare CCD configuration. The red channel has three different Shack-Hartmann lenslet arrays allowing us to accommodate a range of image quality in the SOFIA telescope. The wide glass selection available for the red channel optics allows this optical train to achieve low distortion and excellent image quality while also keeping all optics away from a focus location for the purposes of precise photometry. Relative alignment of the two fields of view is adjustable; the current value is listed in Table 1.

Table 1. HIPO Performance Requirements

Detector	Verification Method	Requirement	Actual
Read noise, 1 Mpx/s	Measurement	6 electrons rms	6 e^- (blue) 15e^- (red) (not yet optimized)
Read noise, 20 Kpx/s	Measurement	3 electrons rms	Not checked yet
Peak quantum efficiency	Vendor measurement	≥80%	82% (blue), 88% (red)
0.35-0.85 micron QE	Vendor measurement	≥40%	42% minimum
Full frame read rate	Demonstration	≥2 Hz (unbinned)	Mode not finished
Three 80x80 subframes	Demonstration	≥50 Hz (3x3 binned)	Mode not finished
One optimal 80x80	Demonstration	≥100 Hz (3x3 binned)	Mode not finished

Filters	Verification Method	Requirement	Actual
Johnson UBVRI	Vendor measurement	Standard bandpasses	Standard bandpasses
Methane filter, 0.89 μm	Vendor measurement	892 nm λ_c, 17-19 nm $\delta\lambda$ ≥80% T_{peak}, 10^{-5} blocking	892 nm λ_c, 17.8 nm $\delta\lambda$ 90% T_{peak}, 10^{-5} blocking

Optics Configuration	Verification Method	Requirement	Actual
Number of channels	Design	Two	Two
Alignment	Measurement	≤ 100 pixels and 1 degree	40 pixels, 0.1 deg (Typ)
Pupil viewing optics	Design	Red, blue, and bare CCD	Red, blue, and bare CCD
Shack-Hartmann optics	Design	Red channel only	Red channel; 3 lenslet sets
Bare CCD, 0.055”/px	Design	Present	Present, with filter wheel

Optical Performance	Verification Method	Requirement	Actual
Unbinned image scale	Measurement/analysis	1/3"/pixel	0.327 (red), 0.331 (blue) "/pixel
3x3 binned image scale	Measurement/analysis	1"/pixel	0.981 (red), 0.993 (blue) "/pixel
Field of View	Measurement/analysis	5.6'x5.6'	5.58' (red), 5.66' (blue)
Image quality	Measurement/analysis	80% encl. light in 2x2 px	80% encl. light < 2.5 pixel diam.
Distortion	Measurement	≤0.1% (red channel), ≤0.3% (blue channel)	Not yet detected Not yet detected
Optics throughput	Measurement/analysis	≥70%, 0.4-0.9 micron	See text in Section 4

Table 1. HIPO Performance Requirements, Continued

Detector Thermal	Verification Method	Requirement	Actual
Detector temperature	Measurement	-100 to -130C	-40C; needs new cold strap
Detector temp. stability	Measurement	±0.5C	±0.2C
Cryostat hold time	Measurement	24 hours	29 hours (lab)
Cryostat cooldown time	Measurement	NA	6 hours (lab)

Time and Position	Verification Method	Requirement	Actual
Time accuracy	GPS vendor spec	50 μs	200 ns (typ)
Position accuracy	GPS vendor spec	30 meters	5 meters (SA off)

Stiffness (HIPO alone)	Verification Method	Requirement	Actual
Flexure	FEA	≤0.1" referred to sky	~0.05"
Lowest resonance		≥100 Hz	
Mirror mounts	Accelerometer		96, 99, 170 Hz
Detector mounts	Spring const. & mass		130 Hz
Optics box	FEA		110 Hz

Sensitivity	Verification Method	Requirement	Actual
Red Channel	Standard Star	NA	See text in Section 4
Blue Channel	Standard Star	NA	See text in Section 4

3. INSTRUMENT DESCRIPTION

3.1. General Discussion

The optimal way to observe an occultation varies widely from event to event. Some have higher time resolution requirements than others, some involve stars with extreme colors or occulting objects with strong spectral features, some involve bright occulting objects while other occulting objects are nearly invisible. Depending on the situation the optimum instrument configuration and data acquisition scheme will vary accordingly. In high S/N cases, it is usually desirable to observe simultaneously at multiple wavelengths, while in low S/N cases a single optimized channel is best. There are strong near-IR spectral features in the atmospheres of the outer planets, and some satellites, so it is can be advantageous to observe at these wavelengths. To complicate matters further, occultations are unique events, so an equipment problem at an inopportune moment may cause the event to be lost entirely. As a result, it is desirable for the instrument to be fault-tolerant and to have a variety of fallback options that can be put in play rapidly and reliably. Finally, the SOFIA test requirements place further demands on the flexibility of the instrument's capabilities.

These considerations have resulted in an instrument that has redundancy designed in and that is highly flexible in terms of optical configuration, electronic operation, and detector readout modes. While flexibility and backup operation modes are generally desirable from an astronomical point of view, they turn out to run counter to the normal way of doing business in the civil aviation world and are thus confusing and somewhat troublesome from the FAA airworthiness point of view. We have therefore had to create a formal scheme for managing and documenting the instrument details and for maintaining rigorous control of all the configurations. Our approach is colored by the fact that the FAA needs insight into only those configuration aspects that have safety implications. Furthermore, it is desirable to include only these things in the FAA documentation in order to simplify the process for future improvements to the instrument. However, everything needs to be defined and controlled for the purpose of documenting the observations made with the instrument. The resulting documentation scheme is therefore somewhat convoluted.

The opto-mechanical layout of HIPO in its most inclusive configuration is shown in Figure 1. For scale, the main mounting flange (labeled 3) is 41 inches from left to right as seen in this top view. Light enters the instrument from the bottom of the page as shown here. The small isolated unit at the bottom of the figure (labeled 1) is an optional sapphire

window located near the large gate valve that is part of the SOFIA telescope. The units mounted on the gate valve side of the main mounting flange form a periscope to direct light into FLITECAM when it is co-mounted with HIPO (see also Figure 2). The optical layout inside the HIPO optical box is described in the caption of Figure 1. The SDSU Gen II CCD controllers are mounted to the side walls of the instrument outside the optical box. Stepping motor driver boards in die-cast aluminum boxes are mounted to the side walls but inside the optical box. These are largely hidden in Figure 1 by angle brackets that stiffen the side plates and provide support for the sliding top cover.

The configuration shown in Figure 1 allows two-channel HIPO operation. Removing dichroic beamsplitter (4) renders the blue channel inoperable but increases the signal available to the red channel. Conversion to the bare CCD configuration involves moving the red dewar and filter wheel so that the red CCD is in the telescope focal plane. Items 4, 5, 8, and 9 must all be removed in this case due to mechanical interference.

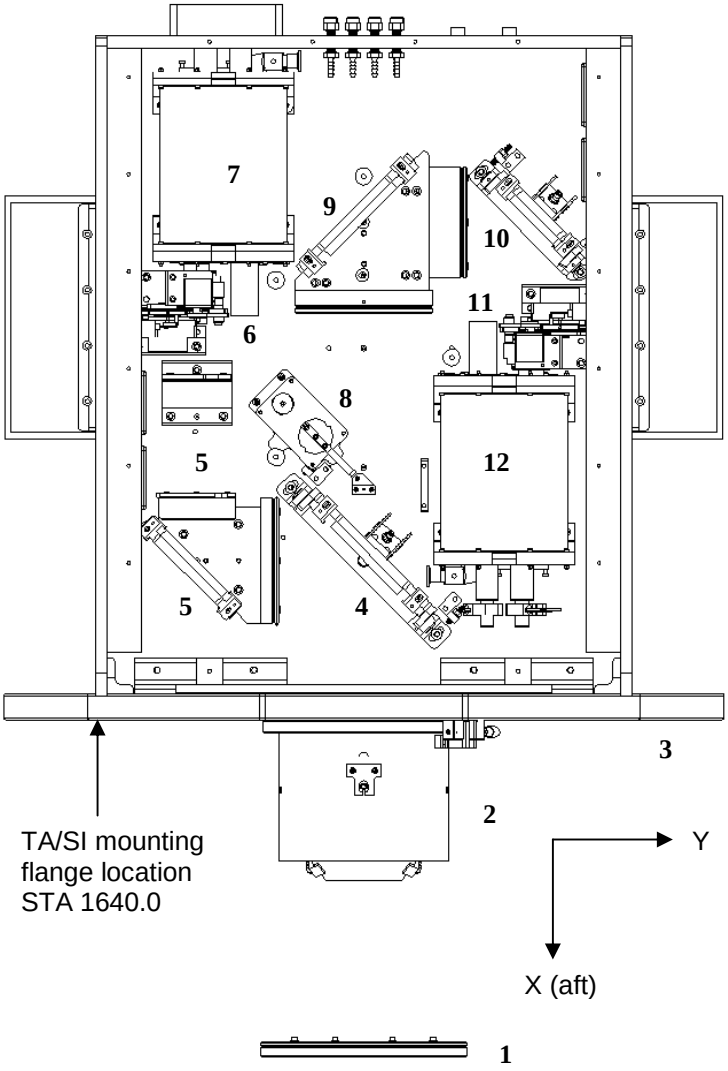

Figure 1: HIPO Internal Configuration.

This figure shows a top view line drawing of HIPO with its cover removed. Light enters the instrument from the bottom of the frame in this view. It first encounters the (optional) gate valve window (1) and the FLITECAM periscope (2) before passing through a window (hidden in this view) mounted in the main mounting flange (3). Depending on the configuration the aircraft pressure boundary includes either the gate valve window or the main mounting flange.

Inside the light-tight HIPO optical box, the beam is split by a dichroic reflector (4). Shorter wavelengths are reflected toward the blue side collimator (5) which is in two parts. The first of these incorporates an aluminized fold mirror with a multiplayer coating that is optimized for its bandpass. The beam finally encounters the filter wheel and camera lens with focus stage (6) and enters the liquid nitrogen cooled blue CCD dewar (7).

The red band transmitted by the dichroic (4) passes the Shack-Hartmann calibration beamsplitter (8) that may be swung in or out of the beam as desired. It then encounters the red collimator with silver-coated fold mirror (9), a second silver-coated fold mirror (10), and finally the red side filter wheel and camera lens assemblies (11) before entering the red CCD's dewar (12).

We noted earlier that it is possible to operate HIPO in conjunction with FLITECAM. Figure 2 shows a side view of this co-mounted configuration. Installation is done by mounting HIPO to the SOFIA telescope first and then mounting the FLITECAM cryostat to the HIPO main mounting plate. After this a support bracket is attached to trunnion mounts on the FLITECAM cryostat and then to the HIPO back plate. This bracket increases the stiffness of the FLITECAM

mount and is not required for airworthiness reasons. The FLITECAM periscope is mounted to the telescope side of the HIPO main mounting plate. It consists of a gold dichroic reflector and a silver-coated fold mirror. This directs the IR beam into the FLITECAM cryostat while transmitting the optical beam to HIPO. There are sufficient tilt adjustments in the periscope to allow simultaneous alignment of the fields of the instruments and pupil alignment in FLITECAM. Focus is achieved by focusing the telescope on the FLITECAM detector and subsequently using the internal HIPO focus mechanisms to accommodate any focus offset between the instruments. This small offset varies depending on the HIPO optical configuration and is designed to be zero in the bare CCD case where HIPO focus adjustment is impossible.

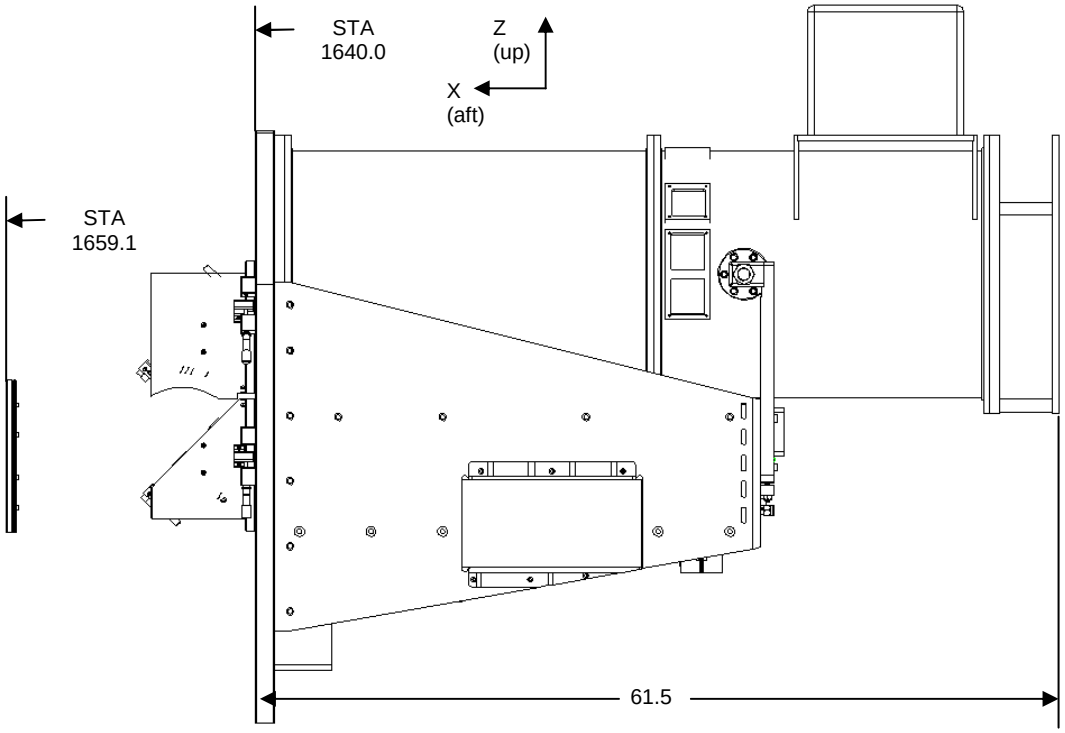

Figure 2: HIPO-FLITECAM co-mounted configuration. This side view shows FLITECAM mounted above HIPO as the pair of instruments would appear with the SOFIA telescope in the center of its elevation range. Light from the telescope enters the instrument from the left. FLITECAM mounts to the main HIPO mounting plate and is also supported by a brace attached to the HIPO end plate. The two units on the telescope side of the main mounting plate are supports for the FLITECAM periscope optics.

3.2. Configurations and Modes

Our organizational approach for dealing with the flexibility of the instrument includes two main categories. We define the word "configuration" to mean an opto-mechanical arrangement of the instrument, including the FLITECAM co-mounting cases. Configuration changes involving relatively large items have FAA visibility while the mechanically minor ones do not. Second, we use the term "mode" to describe the detector operation mode. The modes do not have FAA visibility since all HIPO software, from the airworthiness perspective, is in the "No Effect" class. Modes are identified by names.

3.3. Instrument Configurations

For the purposes of describing the instrument we list in Table 2 the variables that can be changed to produce the various possible major instrument configurations. Refer to Figure 1 to identify the various components involved. When the gate valve window is installed the volume between the gate valve window and the main mounting flange can be held either at cabin pressure or can be evacuated. This region has a very strong thermal gradient in flight, and evacuation will eliminate any possible imaging problems due to turbulence. Converting to the bare CCD configuration involves moving the red CCD dewar so that the CCD is directly in the focal plane of the telescope. The red filter wheel is moved as well and many other components must be removed due to mechanical interference. The product of two FLITECAM conditions, three gate valve window/tub conditions, and three internal HIPO configurations equals a total of 18 distinct major HIPO configurations. These are enumerated on the HIPO top-level drawings.

Table 2. HIPO Instrument Major Configuration Variables

FLITECAM	Gate Valve Window and Tub Environment	HIPO Internal Configuration
Installed	Installed; rough vacuum	Beamsplitter installed – 2 channel operation (Figure 1)
Not Installed	Installed; cabin pressure	Beamsplitter not installed – red channel operation
	Not installed; stratosphere	Bare CCD configuration

Table 3 lists the various minor instrument configurations. The term “low-resolution” refers to the normal configuration with reimaging optics in place while “high-resolution” refers to the bare CCD configuration. The low-resolution pupil viewing lenses are close in size and weight to the camera lenses and can be interchanged easily through access hatches in the top of the instrument. In the case of the bare CCD configuration, the small pupil viewing lens is attached to the retaining ring of the HIPO entrance window. It can also be installed and removed easily through an access hatch. It provides a much higher resolution pupil image than the other pupil viewing lenses can and will be useful in some of the early telescope tests. The Shack-Hartmann configuration is put in place simply by rotating the red filter wheel to a position containing a lenslet module and flipping the calibration beamsplitter into the beam. There are three different lenslet arrays so there are effectively three variants of this configuration.

Table 3. HIPO Instrument Minor Configurations

Configuration Name	Description
Low-resolution 2-channel imaging	Beamsplitter installed, camera lenses in both channels
Low-resolution 1-channel imaging	Beamsplitter removed, camera lens in red channel
High-resolution 1-channel imaging	Bare CCD mode, CCD directly in telescope focal plane
Low-resolution 2-channel pupil viewing	Beamsplitter installed, pupil viewing lenses in both channels
Low-resolution 1-channel pupil viewing	Beamsplitter removed, pupil viewing lens in red channel
High-resolution 1-channel pupil viewing	Bare CCD mode with pupil viewing lens installed
Low-resolution 1-channel imaging and 1-channel pupil viewing	Beamsplitter installed, camera lens in one channel, pupil viewing lens in the other channel. There are two variants of this case.
Shack-Hartmann, 1-channel	Beamsplitter removed, Shack-Hartmann lenslet array in place. There are threee variants of this case.

3.4. Cryogenic System

The two detector dewars (see Figure 3) are identical 3-liter liquid nitrogen dewars. They are mostly aluminum with two separate stainless steel necks and a stainless steel back plate. The dual necks provide a redundant vent path in case there is a problem venting from one of the necks. This was our response to an airworthiness concern regarding possible over-pressurization of a dewar. In a similar vein, there is a relatively elaborate venting system for the boiloff gas from the dewars. This system terminates in four non-return pressure relief valves mounted in the end plate of the instrument

(seen at the top center of Figure 1), two valves for each dewar. The valves are connected to the dewar necks with rubber hoses. The location of the valves at some distance from the dewars greatly reduces the chances that the valves will become stuck due to ice buildup. One valve vents at 2 psi while the other is a 4 psi valve. Under normal operating conditions the 2 psi valve will vent and the 4 psi valve will remain closed. This is expected to be the case even in the event of loss of vacuum in the dewar. The valves perform both a pressure relief function and prevent water vapor from entering the cryogenic area during aircraft descent. They are the central element in the HIPO System Safety Assessment.

The dewar design incorporates two other unusual features. The outer vacuum shell of the dewar includes an O-ring sealed port that is held in place only by air pressure and is captured by long screws. The function of this "falloff" port is to relieve pressure in the event that the internal cryogen can ruptures. The other unusual feature is a set of retaining fingers or hard stops near the ends of the cryogen can. Normally the cryogen can is held in place with four G-10 straps, but G10 is not an analyzable material from the FAA point of view. There must be another, analyzable, means of capturing the cryogen can under the emergency load conditions and the hard stops serve this function.

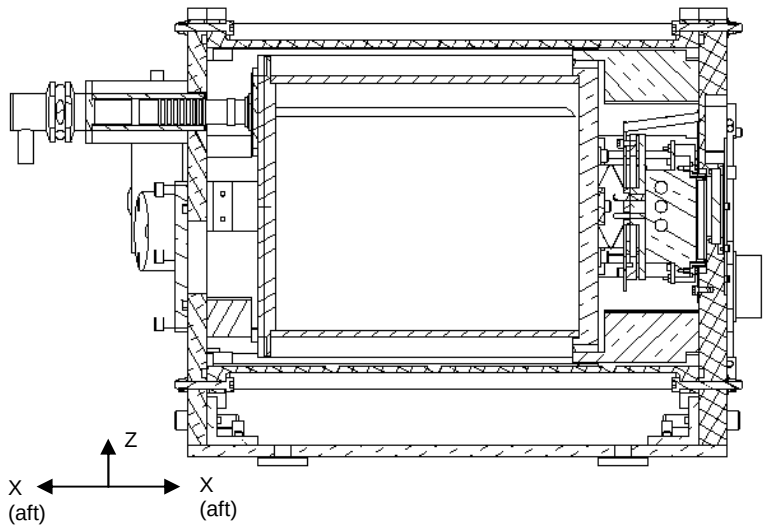

Figure 3: HIPO Dewar Section View

This section view is through the center of the optical path, which is offset from the center of the dewar. The falloff port is located on the end plate (left) and is captured by long cap screws that can be seen protruding to the left. The necks are welded to the end plate and the vacuum valve is also located on this plate. Optional tubes may be installed in the necks so that the dewars can be either up- or down-looking. The front plate (right) includes the window, hermetic connector, and provision for attaching the CCD mounting structure. The spring-type cold strap shown here has inadequate thermal contact and will be replaced with a braid that is attached with screws.

3.5. Electronics

We have implemented the HIPO control electronics with an eye toward reliability, redundancy, and fault tolerance because of the uniqueness of occultation events. The instrument electronics block diagram (Figure 4) shows that HIPO is essentially two independent single-channel instruments. Each channel's instrument-mounted electronics consist of the CCD in its dewar, an ARC (Leach) CCD controller[11] with associated power supply, a filter wheel and focus stage each with a stepper motor controller, a shutter driver, an embedded control computer, a network media converter, and a DC power supply (not shown in Figure 4) for the embedded computer, the motor drivers, and the media converter. The PI rack electronics located on the aircraft floor contains a control computer, GPS-based clock, and network media converter for each channel. The shaded items in Figure 4 (the supervisor computer and network switch) are single-string. We will fly mechanically mounted spares of these units in the event that a failure requires a module-level replacement. The supervisor computer can in fact be replaced by a laptop running an X window server if necessary.

Obviously failure of a single item that is included in both channels' electronics will result in loss of at most a single channel's data. Some failures can be worked around, and these failures will not result in any loss of data. For example if the embedded control computer fails in one channel, timing and motor control can be taken over by the computer for the other channel by a change in cabling. Similarly, the DC power supplies are sized and wired such that a single

supply can operate both channels if necessary. If a shutter driver fails, the shutter is open, and we can operate without it entirely because of the frame-transfer nature of the CCDs. If a motor driver fails we can cross-strap temporarily to the corresponding driver for the other side, or even operate a filter wheel or focus stage by hand.

We will keep spares of most units on hand, but at this time we anticipate that in-flight module replacement will not be allowed for airworthiness reasons. In-flight recabling will be allowed, which is the reason for the emphasis on this approach for dealing with module level failures.

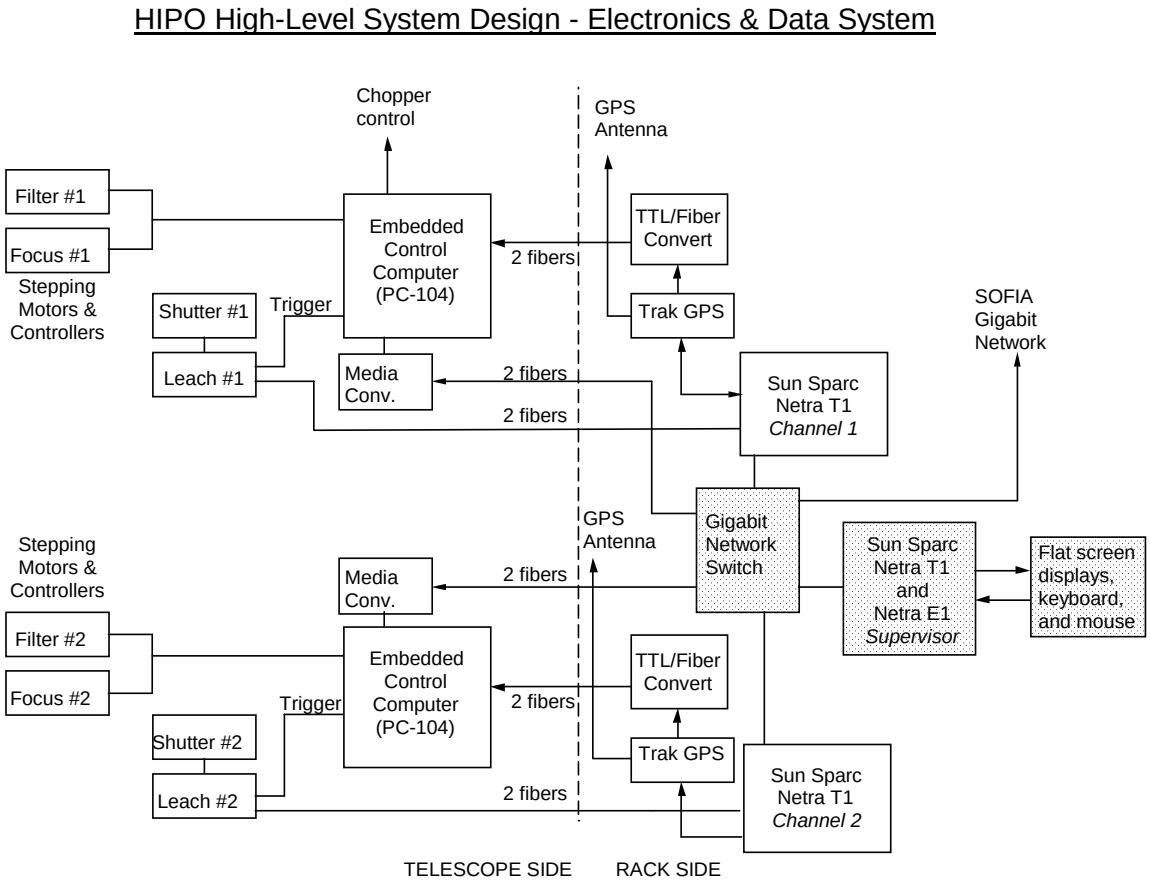

Figure 4: HIPO Electronics Block Diagram. The dual nature of the instrument is easily seen. The shaded blocks are the only items that are not duplicated for each HIPO channel. Power supplies and power connections have been suppressed for clarity. The only connections from the PI rack to the instrument are 12 fibers and two AC power lines.

We have generally used commercial electronic products, although a few small circuit boards were designed in-house. A few of the electronics units deserve further comment. The PC-104 embedded control computers are PCs running Linux on a flash disk. The Sparc Netra computers are 1U rack-mounted units intended for use in the telecommunications industry. They incorporate hot-swappable disks and a single PCI slot. The supervisor computer needs more than one PCI slot, so it includes an expansion chassis. The most unusual feature of these machines is the "Lights-Off-Management" (LOM) port. This allows external control of many low-level functions of the computer, even including power switching.

3.6. Operating Modes and Control Software

HIPO will be operated by the Lowell Observatory Instrumentation System (LOIS)[12, 13]. This is a modular instrument control system built on a core written in C with a TCL/Tk layer for scripting and Graphical User Interface functions. LOIS currently operates a wide variety of CCD cameras at Lowell and elsewhere. The LOIS modules used for HIPO include detector control, instrument control (e.g. focus, timing, filter changing), telescope control, image display, simple real-time analysis, and engineering/test modules. HIPO uses the ds9 image display utility[14] with the X Public Access (XPA) software interface[15]. This allows full use of display scaling and ds9-native analysis functions. LOIS includes a capability to accept commands from another process, either local or remote. We use this interface to allow coordinated operation of the two HIPO channels from the supervisor computer.

The key to HIPO's functionality for time-resolved imaging is its ability to acquire high-speed data that are precisely time-tagged. We achieve this by generating a hardware trigger signal in the embedded control computer that is used to synchronize the activity of the Digital Signal Processor (DSP) on the timing board in the ARC CCD controller. The trigger signal is used in various ways by the several readout modes, but with the final result that the timing details of a given image are known with precision limited by the duration of a tight polling loop in the DSP software, perhaps a few microseconds. At present these modes are defined but only the Single Frames mode has been implemented for HIPO. The Strips mode (also known as time-delay and integrate, or TDI mode) and Slow Dots mode have been implemented in other LOIS-controlled CCD instruments. The following paragraphs describe the modes that HIPO will ultimately incorporate: Find, Single Frames, Series, Basic Occultation, Fast Occultation, Fast Dots, Slow Dots, and Strips.

In Find mode the shutter is opened and the CCD read out repeatedly until interrupted by the observer. This mode is intended as an aid in field acquisition. Generally images obtained in find mode are not stored, although the last image prior to interruption may be manually saved if desired. A string of find mode images is started asynchronously. Images are read out with the desired integration interval unless the requested interval is too short to be possible. In this case images are obtained as rapidly as possible. This mode never uses hardware triggering. An image manually saved in find mode is stored as a single 2-D FITS file with optionally included prescan, postscan, and overclocked pixels. If saved, the file index number is incremented.

Single Frames is a simple imaging mode. In its simplest form it takes a picture and stores it to disk, incrementing the file index number afterwards. It is also possible to request that several frames be taken with one command. These frames are not synchronized in any way – it is intended to be a shorthand way to allow multiple images to be taken. Each image is in a separate sequentially numbered file just as if a single frame were to be taken several times. The images are straightforward 2-D FITS files with optionally included prescan, postscan, and overclocked pixels as described earlier.

In Series mode, a hardware timed, evenly spaced set of shuttered images is obtained. The exposure time of each image is defined by the mechanical shutter. For exposure times equal to or longer than the readout time the basic occultation mode is preferred because the frame transfer can occur more quickly than the mechanical shutter can respond. The images are 3-D FITS files organized as a stack of 2-D images. The third axis is time. Each 2-D image in the 3-D file is stored with optionally included prescan, postscan, and overclocked pixels. These files can become very large. The duty cycle is relatively poor because the dead time per image is the readout time.

Basic Occultation mode is the main high-speed time resolved imaging mode for HIPO. This mode is rigorously timed by using the hardware triggering electronics. The mechanical shutter remains open during the entire time series observation with the frame transfers defining the integration boundaries. This mode is distinguished by the fact that the full 1024 row frame transfer is done at the completion of each integration. There is no preferred location for the object of interest. The maximum frame rate depends on readout details. The images are 3-D FITS files organized as a stack of 2-D images. The third axis is time. Each 2-D image in the 3-D file is stored with optionally included prescan, postscan, and overclocked pixels. These files can become very large.

Fast Occultation mode is a more efficient but more specialized variation of the basic occultation mode. It is rigorously timed by using the hardware triggering electronics. The mechanical shutter remains open during the entire time series observation with partial frame transfers defining the integration boundaries. This mode is distinguished by the fact that only a partial frame transfer (of as many rows as the subframe height) is done at the completion of each integration. At this time the image area begins integrating and the charge image from the previous integration is shifted the rest of the way down to the serial register as the next integration is proceeding. This reduces the dead time due to parallel shifting

compared to the basic occultation mode in the ratio of the subframe height to the 1024 rows in the full image area. There is a preferred location for the object of interest, namely in the first subframe height above the boundary between the image and storage areas. The maximum frame rate depends on readout details. Because only a partial frame transfer occurs, each image is exposed to sky for a longer period than the integration time on the object of interest. This is not a serious issue since this mode will only be used at high frame rates. If necessary a focal plane mask can be introduced to reduce this problem. The images are 3-D FITS files organized as a stack of 2-D images. The third axis is time. Each 2-D image in the 3-D file is stored with optionally included prescan, postscan, and overclocked pixels. These files can become very large.

Fast Dots mode[6] allows acquisition of a finite string of images at very high frame rates using the CCD as an analog storage buffer. The star image should be placed on the CCD near the edge farthest from the serial register. The mechanical shutter is opened, and after every integration interval the parallel clocks are activated to shift the integrated charge image toward the serial register by a number of rows. When the requested number of shifts has been carried out the shutter is closed and the CCD is read out. The integration interval is limited only by the time required to clock the parallels by the number of rows requested. If the file is displayed as a 2-D image it appears to be a string of images (dots) arranged vertically and spaced, on average, by the number of rows shifted between integrations. This is in fact the form of the charge image in the CCD at the time readout is started. We have chosen to represent a fast dots dataset as a 3-D FITS file. It will often be the case for images obtained in this mode that the mechanical shutter's opening and closing times will be very slow compared to the integration interval. This may cause the first images to be faint or entirely missing while the last image may be excessively bright. Also if the integration interval is not much larger than the required parallel shift time, the star images will appear to have streaks connecting them due to charge accumulation during the parallel shifts.

Slow Dots mode produces data similar to the fast dots mode but instead of separating the individual images by parallel shifts only, the images are separated by full readout of the number of rows in the subframe. The result is that slow dots mode can produce an arbitrarily large number of images at the expense of a much longer shifting period. Depending on the details of the readout slow dots will be on the order of 100 times slower fast dots mode. It is important to locate the star of interest in the first subframe height above the boundary between the storage and image areas so that the last charge image is hidden behind the aluminum covering of the storage area after each readout is complete. In order for the individual images to be read out of the CCD correctly, 1024 must be an integer multiple of the subframe height. The data produced by this mode is again a 3-D FITS file. This file will include as many blank frames at the beginning as there are subframe heights in the 1024 rows of the storage area of the CCD.

Strips (or TDI) mode is exactly the slow dots mode with a one-row subframe height. We list this as a separate mode because of the way it is used rather than the way it is implemented. This mode may be useful on SOFIA for testing the telescope scanning operation with the scan direction parallel to the CCD columns. Also, if the image is binned by a large factor in the parallel direction it is possible to obtain a high-speed one dimensional star position over long time periods. Finally, if a coarse grism is incorporated in the HIPO optical system along with an aperture at the focal plane, a spectrally resolved time series can be obtained at high speed. This would be appropriate for observing lunar occultations.

4. AS-BUILT PERFORMANCE

One of the largest areas of concern for the SOFIA telescope is pointing stability. A related concern revolves around the stability and performance of the telescope's servo control system. It is desirable to have all the vibrational modes of the instrument at higher frequencies than telescope modes that have an impact on the controller. Since HIPO will be a key tool for measuring pointing stability, it was clear at the outset that our mechanical design would have to be robust enough that HIPO would not be a significant image motion contributor or have an adverse impact on the servo system.

Consequently, we arranged to have a substantial finite element analysis (FEA) done by Eugene Loverich from Northern Arizona University. Several modifications to the original mechanical concept were made in order to increase the lowest vibrational mode frequency and to limit the flexibility of the instrument. These included moving the CCD controllers so their centers of mass are in line with the heavy HIPO optical table, adding stiffeners to the side plates, adding support posts in strategic locations to tie the top of the optical box to the optical table, and making the main mounting plate thicker. The result is that the lowest HIPO-only vibrational mode is at about 110 Hz, well out of the realm of control system complications. Its maximum deflection under the differential gravitational load expected in flight is consistent

with measuring image motion at the original specified value of 0.2 arcseconds. The FEA also included analysis of an external representation of the FLITECAM cryostat. The FLITECAM model had the correct mass, center of gravity, and wall stiffness, but had no knowledge of structure inside the cryostat. The lowest modes for the co-mounted cases were in the vicinity of 65-70 Hz, but internal modes will likely be lower. For practical reasons, the actual attachment of the support bracket to the cryostat is less satisfactory mechanically than the modeled attachment.

The FEA was for the main HIPO structure and did not include detailed modeling of optical or CCD mounts. These were fabricated first and then tested. The detector mount was loaded and the resulting deflection measured with a dial indicator. A conservative resonant frequency was calculated based on the resulting spring constant and the total mass of the mount. The beamsplitter and mirror mounts were measured directly with an accelerometer. As shown in Table 1, the frequencies are all near or above 100 Hz.

The optical design of HIPO accommodates all of its requirements[9]. The as-built performance of the HIPO optics is in excellent agreement with the design expectations with the possible exception of the image quality (see below). The final design iterations accounting first for test plate fitting and finally for the as-built lens thicknesses and radii resulted in a slight change in effective focal length and image scale (see Table 1). Distortion is small enough that the first approach we used to measure it in the lab was unsuccessful. We will characterize it using star field images and accurate star catalog positions.

We measured the image quality of the HIPO reimaging optics using the HIPO detectors. This was somewhat problematic due to the small design image size and to sources of image quality degradation other than the optics under test. Our test source was an artificial star projector based on a spherical mirror operating slightly off-axis. The astigmatism in the resulting image was comparable to the quality we were trying to measure. In addition, CCDs suffer image blurring due to charge diffusion in the detector that is on the order of a pixel. Both of these blurring effects had to be removed from the observed PSF to estimate the optical performance alone. Our best estimate is given in Table 1, an 80% enclosed light diameter of 2.5 pixels or about 0.8" on the sky, about 25% worse than the requirement.

The design of the camera lenses included an adjustable decenter correction on one element in the red camera lens and two elements in the blue lens. The adjustment approach worked well in the red lens, but the two-element adjustment of the blue camera lens was too difficult to deal with in practice. The two adjustments were independent but only if images at the field center and field edge could be optimized simultaneously. If an on-axis image was optimized alone, the two adjustments were highly correlated. The practical solution was to mechanically center the element that had the weaker effect on image quality and then optimize the other element using an on-axis image.

We have approached measurement of the instrument's throughput in two ways so far. First, we have made a model of the transmission and reflection of all the optical surfaces and the CCD quantum efficiency. All of these curves were based on vendor-supplied data. Second, we observed spectrophotometric standard stars[16] using the 1.8-meter Perkins telescope to determine the actual detected signal level in electrons per second. We did not measure atmospheric extinction on the nights when the standards were observed, but used normal extinction values for Lowell. The telescope was freshly aluminized before the first observations, so we used a bare aluminum surface reflectivity curve in our model for the two mirrors in the telescope. The observed standard star signal is lower than the predicted signal by approximately 20-30%, with the blue side possibly having lower throughput than the red side. It is not clear at this time if the discrepancy is due to extinction, telescope coating reflectivity, an error or misunderstanding regarding the coating transmission curves, or some combination of all of these items. An end-to-end test of most of the optics taken as a whole will be done in the lab by comparing the signal measured in the bare CCD configuration with the signal seen through the reimaging optics.

HIPO includes ancillary optical capabilities including pupil viewing, Shack-Hartmann testing, and a retro-reflection capability. To date the pupil viewing lenses for the red and blue side reimaging optical systems have been used and function as expected. We have recently added the capability to image the pupil using the bare CCD configuration, which results in a very high resolution pupil image. The parts for this have been made but this configuration has not yet been tested. The Shack-Hartmann optics have been used with all three MLMs, and the resulting images are formed as expected from the design. We have not yet characterized the accuracy of the aberration determination because the analysis software is not yet complete. Finally, the retroreflection light source has been tested, and the spherical mirror has been fabricated, but we have not yet had an opportunity to test HIPO with the spherical mirror.

5. ACKNOWLEDGEMENTS

HIPO development is supported under USRA Grant 8500-98-003. We owe a debt of gratitude to the Lowell Observatory technical staff for their work in support of this project. In particular, we thank Ralph Nye and Jim Darwin for their tireless efforts with the mechanical drawings and machining work, and their willingness to adapt to the FAA approach to these activities. We also wish to thank Lowell's Director, Bob Millis, for his unwavering support of the project. Finally, we apologize to the scientific staff of the Observatory for the lengthy delays in many other projects that resulted from the unexpectedly large amount of work required for HIPO development.

6. REFERENCES

1. Elliot, J.L., "Stellar Occultation Studies of the Solar System", *Ann. Rev. Astron. Astrophys.* **17**, 445-475 (1979).
2. Dunham, E.W., and J.L. Elliot, "Optical Photometry with the Kuiper Airborne Observatory", *Pub. A.S.P.* **95**, 325-331 (1983).
3. Dravins, D., L. Lindegren, E. Mezey, and A.T. Young, "Atmospheric Intensity Scintillation of Stars. I. Statistical Distributions and Temporal Properties", *Pub. A.S.P.* **109**, 173-207 (1997).
4. Charbonneau, D., T.M. Brown, D.W. Latham, and M. Mayor, "Detection of Planetary Transits Across a Sun-like Star", *Ap. J. Let.*, **529**, L45-L48 (2000)
5. Brown, T.M.., and R.L. Gilliland, "Asteroseismology", *Ann. Rev. Astron. Astrophys.* **32**, 37-82 (1994).
6. Dunham, E.W., R.L. Baron, J.L. Elliot, J.V. Vallerga, J.P. Doty, and G.R. Ricker, "A High Speed, Dual-CCD Imaging Photometer", *Pub. A.S.P.*, **97**, 1196-1204 (1985).
7. Elliot, J.L., *et al.*, "Image Quality on the Kuiper Airborne Observatory. I. Results of the First Flight Series", *Pub. A.S.P.* **101**, 737-764 (1989).
8. Dunham, E.W., J.L. Elliot, and B.W. Taylor, "HOPI – A High-Speed Occultation Photometer and Imager for SOFIA", *Proc. SPIE* **4014**, 76-84, (2000).
9. Dunham, E.W., "The Optical Design of HIPO: A High-speed Imaging Photometer for Occultations", *Proc. SPIE* **4857**, 62-72, (2002).
10. Horn, J.M.M., E.E. Becklin, O. Bendiksen, G. Brims, J. Goulter, E. Kress, N. Magnone, I.S. McLean, J. Milburn, N. Molayem, H.S. Moseley, and M. Spencer, "FLITECAM – A near-infrared camera for test and science applications on SOFIA", *Proc. SPIE* **4014**, 64-74, (2000).
11. Leach, R.W., F.L. Beale, and J.E. Eriksen, "New-generation CCD controller requirements and an example: The San Diego State University generation II controller", *Proc. SPIE* **3355**, 512-519 (1998).
12. Taylor, B.W., E.W. Dunham, A. Gould, D.J. Osip, and J.L. Elliot, "Lowell Observatory Instrumentation System (LOIS): A Modular Control System for Astronomical Instrumentation", *Proc. SPIE* **4009**, 435-442, (2000).
13. Taylor, B.W., E.W. Dunham, and J.L. Elliot, "A critical review of the Lowell Observatory Instrumentation System", *Proc. SPIE* **5496**, (5496-50, these conferences), (2004)
14. Joye, W.A. and E. Mandel, "New Features of SAOImage DS9", in "Astronomical Data Analysis Software and Systems XII", Eds. H.E. Payne, R.I. Jedrzejewski, and R.N. Hook, *ASP Conference Series*, **295**, 489 (2003).
15. Mandel, E., R. Swick, and D. Tody, "The X Public Access Mechanism", Proceedings of the 9th X Technical Conference, January 1995.
16. Massey, P., K. Strobel, J.V. Barnes, and E. Anderson, "Spectrophotometric Standards", *Ap. J.* **328**, 315-333, 1988.